JOURNAL OF GEOPHYSICAL RESEARCH, VOL. 106, NO. C1, PAGES 991–1003, JANUARY 15, 2001

On the shape and widening of salt marsh creeks

Sergio Fagherazzi

School of Computational Science and Information Technology, Florida State University, Tallahassee

David Jon Furbish

Department of Geological Sciences and Geophysical Fluid Dynamics Institute, Florida State University, Tallahassee

Abstract. We have developed a model that simulates aspects of initial channel formation in a youthful salt marsh environment. The model mimics the evolution of the cross section of a channel by coupling calculations of bottom shear stresses caused by tidal motions with erosion, taking into account the deposition of cohesive sediments. The simulations characterize flow in a reference cross section that includes an incipient channel zone and a marsh surface zone, with assigned water surface level and initial bottom elevation. This model mimics key characteristics of salt marshes where discharges due to tidal motion repeat in time with approximately the same magnitude and water surface level. Significant reductions in the tidal prism due to increasing bottom elevation above mean sea level, however, are not treated. Rather, the model is suitable for youthful salt marshes where relatively large water depths are maintained. Prolonged deposition reduces the area available for flow and thereby changes the shear stress distribution at the bottom, leading locally to erosion and alteration of the channel cross section. The simulations suggest that two mechanisms contribute to the longitudinal widening exhibited by salt marsh channels, which typically is disproportionately greater than that exhibited by river channels. The short duration of the maximum discharge (spring tide) and corresponding erosion rates, when compared with deposition rates, prevent the channel from reaching a deep, narrow equilibrium configuration. Furthermore, autoconsolidation of cohesive sediments, often occurring in salt marsh environments, leads to a downward increase in the resistance of the sediment to erosion. As scour occurs locally, the flow encounters more resistant sediment layers; so rather than deepening the channel over a narrow zone, flow and bottom stresses become more uniformly distributed leading to a wider channel than would otherwise occur in the absence of autoconsolidation. Based on flow and sediment properties estimated for the Venice Lagoon, Italy, simulations are consistent with observations of salt marsh creeks at this location.

1. Introduction

Salt marshes are composed of an intertidal surface dissected by a network of tidal creeks. The creek network supplies water and sediments to the salt marsh surface, and for this reason it is of fundamental importance to the morphological and ecological evolution of the entire salt marsh. A salt marsh surface is flooded regularly by tides, but it may also be subject to stronger flows caused by storm surges. Creeks, due to a seaward increase in discharge, become deeper and wider seaward with concomitant changes in width-to-depth ratios.

Many studies has been conducted to describe salt marsh hydrology [*Redfield*, 1972; *Pestrong*, 1965; *French and Stoddart*, 1992], salt marsh evolution [*Allen*, 1997, 1995, 1991; *French*, 1993; *Krone*, 1987], sediment deposition on salt marsh surfaces [*Woolnough et al.*, 1995] and the influence of salt marsh vegetation on channel migration and morphology [*Garofalo*, 1980]. Only a few, however, have focused on the shape of salt marsh creeks. In recent years, zero-dimensional and time-stepping numerical models have been developed to describe the vertical growth of salt marsh platforms [*Krone*, 1987; *Allen*, 1991, 1995; *French*, 1993]. These models describe the influence of sediment supply, tidal regime, and sea level movements on salt marsh elevation. The three-dimensional structure of the salt marsh, however, can not be neglected. The hydrodynamics and sediment transport on salt marsh surfaces are inherently linked to tidal creeks; in a feedback process the creek cross-sectional shape and stability are influenced by the flow entering the salt marsh [*Friedrichs*, 1995].

Allen [1997] recognized the importance of the channel three-dimensional structure for the morphostratigraphy of salt marshes and sketched a conceptual model by combing zero-dimensional models with regime theory of channel stability. In this paper we explore the possibility of using a similar approach to describe creek shape. We describe a cross-sectional model that follows the evolution of a salt marsh creek during salt marsh evolution. The model applies to

Paper number 1999JC000115.
0148-0227/01/1999JC000115$09.00

youthful marshes growing upward from tidal flats on a timescale of decades. Our results are consistent with reported field evidence [*French and Stoddart*, 1992; *Gardner and Bohn*, 1980] for youthful salt marshes.

Our work involves coupling a simplified hydrodynamic model based on the continuity equation [*Boon*, 1975; *Pethick*, 1980; *Rinaldo*, 1999b] with recent developments pertaining to river cross-sectional stability [*ASCE Task Committee on Hydraulics, Bank Mechanics, and Modelling of River Width Adjustment*, 1998a, 1998b; *Kovacs and Parker*, 1994; *Diplas and Vigilar*, 1992; *Pizzuto*, 1990].

We consider evolution of a symmetric cross section, neglecting the possibility of spatial variations in flow and sediment transport within the section, which can lead to bars and meanders in terrestrial rivers [e.g., *Blondeaux and Seminara*, 1985]. Thus, although meanders are evident and well documented in salt marsh systems [*Gabet*, 1998], for simplicity we do not describe their possible effects on channel evolution.

Because salt marshes typically involve cohesive sediments, we then adopt a threshold shear stress condition for erosion and channel morphological equilibrium, a common approach in the literature pertaining to cohesive sediments [*Mehta et al.*, 1989; *Parchure and Mehta*, 1985; *Dyer*, 1995]. This threshold stress condition for cohesive sediments greatly simplifies the evolution model. In the case of cohesionless material a force balance on sediment particles has to be considered, leading to a vectorial bedload formulation for sediment transport [e.g., *Kovacs and Parker*, 1994].

Once a channel is formed, erosion is assumed to occur only on the bed sediments, and bank stability with respect to mass failure is not taken in account. For cohesive banks, failure can occur with increasing bank height or slope angle through lateral erosion of the toe of the bank [*ASCE Task Committee on Hydraulics, Bank Mechanics, and Modelling of River Width Adjustment*, 1998a]. Typical depths of salt marsh creeks considered (~ 2 m) suggest the second as the most likely mechanism for bank failure in contrast with rotational failure. *Gabet* [1998] reported cantilever collapses as a result of bank undercut, with the erosion at the toe originating from secondary flow induced by channel sinuosity. An identical failure mechanism has been described for the erosion of the salt marsh margin associated with wind waves and currents [*Van Eerdt*, 1985]. In our model, however, secondary flows due to meanders, wind waves, and currents are neglected; thus we do not consider bank failure in this first analysis.

A further simplification introduced in this paper corresponds to the assumption of spatially uniform sediment deposition. This hypothesis is consistent with zero-dimensional models and leads a flat salt marsh surface. The model is thus suited to depositional environments, such as salt marshes, whose limited topographical area reduces spatial variations in sedimentation rates. The model is not applicable to other tidal environments, like lagoons and estuaries, in which mechanisms in addition to simple deposition lead to channel formation and evolution. In tidal basins sediment exchanges between the major components (tidal flats, salt marshes, and channels) are a key factor for geomorphological equilibrium, whereas sediment availability influences the evolution of estuaries [*Lanzoni and Seminara*, 1998b].

Tidal creeks differ geomorphologically from terrestrial rivers in that channel width varies longitudinally more rapidly than depth. The relatively larger control of increasing discharge on width is reflected well in applications of hydraulic geometry on tidal creeks [*Myrick and Leopold*, 1963]. Hydraulic geometry links width and average depth of the channel in the downstream direction with bankfull discharge:

$$d \propto Q^f \tag{1}$$

$$w \propto Q^b \,, \tag{2}$$

where Q is the discharge, w and d are respectively the channel width and depth, and b and f are the hydraulic geometry exponents. Based on field measurements, b and f vary around average values of 0.50 and 0.49 in terrestrial rivers, respectively [*Leopold and Maddock*, 1953], whereas their values for tidal channels are around 0.77 and 0.33 [*Myrick and Leopold*, 1963; *Redfield*, 1972; *Pestrong*, 1965]. This suggests that different geomorphic mechanisms are acting in tidal channels in order to reach the final cross-sectional shape. A larger width exponent suggests that increasing discharge in the downstream direction has a stronger control on the width of the tidal channel than on its depth.

We illustrate two possible mechanisms which are responsible for the larger changes in channel width relative to channel depth; namely, the short duration of the discharge peaks and the autoconsolidation of cohesive sediments [*Cahoon and Reed*, 1995]. Further developments regarding morphological channel equilibrium in mature salt marshes and the presence of vegetation are addressed elsewhere. Our goal is to construct a numerical model that simulates the morphodynamic evolution of a salt marsh. Of significant help toward this end is the recent characterization of planimetric characteristics of the creek network, specifically, the procedure for watershed delineation of salt marsh creeks and the statistical properties of channel branching and aggregation [*Fagherazzi et al.*, 1999; *Rinaldo et al.*, 1999a, 1999b].

2. Flow and Sediment Erosion Models

2.1. Tidal Discharge

Tidal motion in a salt marsh or tidal flat environment is complex. The bed friction and the tapered shape of the channels play a major role in tidal propagation and the related discharge field [*Lanzoni and Seminara*, 1998a; *Friedrichs and Aubrey*, 1994]. Moreover, the spatial complexity of wetting and drying of salt marsh surfaces influences velocities and tidal water levels. To comprehensively model this processes is difficult; for example, the divides of salt marsh channels during flooding are dynamical features associated with the free-water surface such that energy slopes, rather than bottom slopes, determine water trajectories [*Rinaldo et al.* 1999a]. In focusing on the evolution of the cross-sectional shape of a channel due to tidal motion, we therefore adopt a simple model for the tidal discharge that contains essential characteristics of the tidal flow. Namely, we describe discharge as a function of tidal stage based on the continuity model of *Boon* [1975] and *Pethick* [1980]. For a tidal marsh system with a channel closed at one end, we thus suppose that (1) it is possible to delineate the tidal flat area A pertinent to the branched channel (i.e., we can draw the divides associated with the channel) which does not change with time or water level, (2) the area A is strictly linked with the cross section S at the channel mouth, that is, the flow section at the mouth conveys all water entering or leaving the tidal area A, and (3) the free-water surface is uniformly level, that is, the water level at every point of A is equal to the tidal stage at the section S.

Following these assumptions, the continuity equation becomes

$$Q = \frac{dV}{dt} = A\frac{dh}{dt} \ , \tag{3}$$

where Q is the discharge flowing through the section studied, A is the planimetric area of salt marsh (watershed) pertinent to the channel section, V is the total volume of water present on area A, and $h(t)$ is the tidal level. Utilizing this model, *Boon* [1975] demonstrated a very good agreement between simulated and measured tidal prisms (the volume of water flowing in the channel section during flood). Nonetheless, *Healey et al.* [1981] recognized that (3) cannot describe the asymmetry of the water stage-velocity relation in a tidal channel, an asymmetry documented by *Myrick and Leopold* [1963], among others. This asymmetry is due mainly to the lag in the propagation of the tide in shallow waters [*Rinaldo et al*, 1999b]. For salt marshes it also is due to deformation of the tidal wave caused by wetting and drying of the salt marsh surface during high tide, variations in the watershed area with time, draining of small creeks during low tide, and effects of the tapered geometry of tidal channels. It is possible in principle to use (3) taking into account the influence of wetting and drying of the salt marsh surface by considering a "wetted" area function $A(h)$ of water elevation. Following *Rinaldo et al.*, [1999b], however, when we calculate the discharge Q, we do not consider in the calculation the zones of A that are dry at any instant.

It is interesting to note that (3) has been extensively used in the past to model the hydraulic behavior of tidal inlets. By considering the level of the water to be spatially uniform over the basin, A becomes the area of the basin itself, while h is the forcing tide at the basin inlet. This equation is then coupled with the momentum equation describing the flow through the inlet [e.g., *Bruun,* 1978]. In this context, application of (3) is straightforward. All the water entering or leaving the basin has to pass through the inlet. Applying the continuity model to a channel position inside the basin, in contrast, presupposes knowledge of the basin area pertinent to the channel section, an area that can change with time. Moreover, flow may not be confined within the channel but can occur on the tidal flat or salt marsh surface. For mature salt marshes with surface elevations higher than mean sea level (MSL), however, flow velocities over the salt marsh surface typically are 2 orders of magnitude smaller than in the channel [*Lynn et al.*, 1995].

Whereas (3) does not characterize details of salt marsh hydrodynamics, the model nonetheless can be usefully applied in geomorphic studies of salt marsh creeks [*Rinaldo et al.*, 1999b]. Moreover, because we focus on channel cross-sectional shape without taking into account the planimetric geometry of the tidal flat and embedded channel network, we assume that (3) provides an adequate approximation of discharge for a youthful salt marsh. Namely, if the level of the salt marsh area is below the low-tide water level, there is always water at each point within the salt marsh considered, and A becomes constant, independent of water elevation h and bottom topography. This means that the discharge at a specified channel section depends only on the constant area A and the temporal variation of water level $h(t)$. In particular, given a harmonic tidal signal (for example, a semi diurnal tidal wave), the maximum discharge will repeat itself at fixed intervals (neglecting detailed effects of bottom topography). Again, this is consistent with studies of tidal inlets. If the water surface is spatially uniform and the basin is entirely wetted, the discharge at the inlet becomes a solution of a second-order equation (with harmonic boundary conditions), where maximum peaks repeat in time independently of bathymetry (albeit possibly depending on inlet geometry) [*Bruun*, 1978].

It is noteworthy that bottom topography nonetheless is important. Topography influences the propagation and attenuation of waves in a basin. Thus in appealing to the idea that the water level is spatially uniform, we neglect the tidal lag due to finite celerity of the tidal wave and its attenuation due to friction at the bottom. The geometry of the basin as well can influence the motion, leading to reflection and resonance effects. For example, *Maas* [1997] demonstrated that, for the tidal basin inlet problem, the discharge is strongly influenced by bottom elevation when part of the basin becomes dry during the tidal cycle. These phenomena, however, become negligible for short (with respect to the tidal wavelength) and deep basins [*Rinaldo et al.*, 1999a; *Shuttelaars and De Swart*, 1996].

When the elevation of the salt marsh surface increases due to sedimentation, the bottom topography again becomes important. Namely, the volume of water stored on the salt marsh area decreases if part of the salt marsh surface becomes dry during a tidal cycle. As a consequence, discharges in tidal creeks are reduced.

Summarizing, the continuity model through (3) states that, considering harmonic changes in water elevation as a boundary condition and a salt marsh level sufficiently less than mean sea level, the discharge flowing in each section of the tidal creek can be considered harmonic as well.

In particular, the peak discharge repeats at fixed time interval and fixed water elevation with constant magnitude. Assuming that the peak discharge is the geomorphological agent responsible for erosion in the salt marsh environment, our evolution model will utilize an intermittent discharge with constant magnitude to mimic the saltmarsh hydrodynamics.

2.2. Shear Stress Conditions at the Bottom of the Salt Marsh

Knowing the discharge and water depth, it is possible to calculate bottom shear stresses, following recent developments for river width adjustments [*ASCE Task Committee on Hydraulics, Bank Mechanics and Modelling of River Width Adjustment*, 1998a]. In particular, we utilize the numerical model developed by *Pizzuto* [1990] where, for a given gently curved bottom topography, it is possible to use the modified area method [see *Lundgren and Jonsson*, 1964] to find bottom shear stresses. After dividing the wetted perimeter into segments dP, normals associated with each point separating the segments are determined. The local boundary shear stress τ_0 is defined by

$$\tau_0 = \rho g S \frac{dA}{dP} + \frac{d}{dP}\int_0^{D_N} \tau_{\zeta s} d\eta \ , \tag{4}$$

where ρ is the water density, S is the energy slope, dA is the area between the normals to the bed, D_N is the total distance along a normal from the bed to the water surface, η is a spatial coordinate along the normal, and $\tau_{\zeta s}$ is the shear stress acting on planes orthogonal to ζ and directed downstream. It is important to notice that, in contrast to steady flow in rivers, here the flow is unsteady and the water surface (or bottom) slope has to be replaced by the energy slope [*Henderson*, 1966]. In our morphological model we consider a constant discharge that is not directly linked to bottom topography. The energy slope is adjusted only to allow the necessary flow in the considered section. In reality, velocities, energy slope and harmonic boundary conditions are strongly linked with each other through the equations of motions (e.g., the shallow-water equations [*Dronkers*, 1964]). However, the aim of this paper is not to resolve the flow field in a salt marsh caused by tidal motion but rather to provide a simple geomorphological model that simulates cross-sectional shapes of tidal channels.

Through a gradient transport hypothesis it is possible to define the shear stress acting on normals:

$$\tau_{\zeta s} = \frac{\rho\varepsilon}{h}\frac{\partial u}{\partial \zeta} \ . \tag{5}$$

Here ε is the eddy viscosity, u is the local velocity, ζ is the coordinate perpendicular to η, and h is a metric coefficient that takes into account uneven distances between adjacent normals. In particular, $h\zeta$ is equal to dP at the bottom [*Pizzuto,* 1990].

We further suppose, in agreement with rivers, that the velocity profile is logarithmic:

$$u = \frac{u_*}{k}\ln\left(\frac{\eta}{K_S}\right), \tag{6}$$

where k is the von Karman constant and u_* is the local shear velocity defined by:

$$u_* = (\tau_0 / \rho)^{1/2} \ . \tag{7}$$

Whereas the local roughness length K_S for noncohesive material is linked to the grain-size distribution [e.g. *Einstein,* 1950], in this paper we are concerned with fine-grained cohesive sediments, which typically occur in salt marsh environments. Field data nonetheless indicate that a logarithmic profile correctly describes measured velocity profiles in the estuarine environment [*Dyer*, 1970; *Collins et al.*, 1998]. Using regression analysis it is therefore possible to determine the effective roughness length K_S. (For the simulations described below, we adopt a value K_S = 0.003 cm, consistent with reported data [*Collins et al.*, 1998]).

Following *Lundgren and Jonsson* [1964], *Pizzuto* [1990] and *Kovacs and Parker* [1994], the eddy viscosity is assumed to be distributed parabolically along normals to the bed:

$$\varepsilon = ku(\eta - K_S)\left(1 - \frac{\eta - K_S}{D_N - K_S}\right) . \tag{8}$$

Rearranging (4), *Pizzuto* [1990] arrives at an expression for the bed shear stress:

$$\tau_0 = \rho g S \frac{dA}{dP} + \frac{d}{dP}\left(B\frac{d\tau_0}{dP}\right), \tag{9}$$

where B is given by

$$B = \int_{K_S}^{D_N} \frac{1}{2}(\eta - K_S)\left(1 - \frac{\eta - K_S}{D_N - K_S}\right)\ln\left(\frac{\eta}{K_S}\right) d\eta \ . \tag{10}$$

We refer to *Pizzuto* [1990] for the numerical solution of this problem.

The previous formulation, in particular the logarithmic velocity profile, is valid for small curvature of the bed. Moreover, it does not take into account secondary currents and the three-dimensional structure of the flow near the banks. In the simulations presented below, we start with a flat bottom; this leads to a concave channel profile with two convex banks. The evolution thus leads to flow over a compound section whose stress field ultimately deserves more detailed attention [see *Shiono and Knight*, 1991]. Nonetheless, we adopt this formulation for simplicity, as it captures basic characteristics of the process.

To resolve (10), we must apply boundary conditions. Without loss of generality we suppose that the channel evolves symmetrically about an axis, then study half of the cross section. Symmetry leads to the following condition at the channel axis:

$$\frac{d\tau_0}{dP} = 0 \qquad x = 0 \ . \tag{11}$$

In addition, we choose a characteristic transverse length L to define the area through which flow occurs. The endpoints of L, however, are not associated with physical boundaries like banks. Rather, $\pm L/2$ define positions of symmetry separating flow zones centered on incipient channel axes, such that a second boundary condition is

$$\tau_0 = \rho g S y \qquad x = L/2 \ . \tag{12}$$

It is interesting to note that during channel evolution this boundary condition has little effect on the stress distribution over L, but it influences the stress near $x = L/2$. If we alternatively assume as a second boundary condition that $\tau_0=0$ ($x = L/2$), the resulting channel development is the same.

We choose the length L to describe the flow redistribution in the channel and the adjacent salt marsh, with concentration of flow from the salt marsh to the channel. A large portion of salt marsh is for this reason taken in account, and the major part of it remains flat during the salt marsh evolution.

2.3. Erosion and Deposition Conditions

The bottom sediment is assumed to be cohesive. For the erosion we consider the equation:

$$E = M\left(\frac{\tau_0 - \tau_c}{\tau_c}\right) \tag{13}$$

where τ_0 is the bottom shear stress, τ_c is a critical shear stress required for erosion of cohesive sediment, and M is a constant which varies with the type of sediment. This equation assumes that the erosion rate E increases with excess shear stress.

Whereas this equation is valid for homogeneous material, in reality, vertical changes in strength properties of cohesive sediments due to consolidation are common, even over only a few centimeters of sediment depth. Theoretical studies have been devoted to explain these vertical differences. For example, *Hayter* [1986] reported a numerical model to simulate vertical changes in sediment properties, and *Ariathurai and Krone* [1976] utilized a layered-bed model in a numerical simulation of sediment transport in estuaries. For such stratified material, a logarithmic expression may provide a better fit to experimental data [*Parchure and Mehta*, 1985; *Kuijper et al.*, 1989]:

$$\ln\frac{E}{E_f} = \alpha\sqrt{\tau_0 - \tau_c}\ , \tag{14}$$

where E_f and α are constants depending on the type of cohesive material. Simulations involving effects of sediment stratification are described below. Meanwhile, we first consider the simple case of homogeneous bottom sediments using (13). Moreover, as shown by *Sanford and Halka* [1993], a linear relation between erosion rate and shear stress is a good approximation, even with stratification, if the range of shear stresses is small.

The critical shear stress τ_c varies with sediment composition. For clay and silty clay it depends on, among other factors, dry density, plasticity index, void ratio, clay minerals present in the sediments and chemical composition of the flowing water [*ASCE Task Committee on Erosion of Cohesive Materials Committee on Sedimentation,* 1968]. It is also important to note that, when considering empirical relationships linking the critical stress with sediment density [*Delo*, 1988] for cohesive soils, the critical stress may be an order of magnitude larger than the critical stress measured in flume experiments [*Parchure and Mehta*, 1985; *Kuijper et al.*, 1989]. This ambiguity reflects the difficulties involved in estimating the critical shear stress for cohesive materials and points to the need for further laboratory and field measurements addressing this issue.

The evolution of a salt marsh is strongly related to sediment deposition on the salt marsh surface. The deposition rate, in turn, depends on the salt marsh elevation and typically involves an asymptotic curve [*Pethick*, 1981]. Namely, with the hypothesis of an input of sediment at constant concentration, the decreasing deposition rate with time is due mainly to a decrease in tidal inundation of the salt marsh surface [*Allen*, 1997; *French*, 1993; *Krone*, 1987]. In this paper, because we examine only youthful salt marshes with surfaces below MSL, it is reasonable to assume the deposition rate as constant. This hypothesis is consistent with a constant-concentration boundary condition (although in detail the deposition rate may depend on the bottom shear stress [e.g., *Krone*, 1993]).

3. Simulations

Our evolution model starts from a deep flat basin where deposition is occurring at a specified rate. The channel network is not yet developed. However, an exchange of water between the area considered (in the vicinity on an incipient channel) and the rest of the basin occurs so that the water level is equal to the forcing tidal condition at the seaward boundary. With an initial increase in the bottom elevation due to sedimentation, flow may begin to locally scour the deposited sediments to form a channel network. While the channel is forming, the flow becomes increasingly confined and unidimensional, mainly within the channel. In order to start the erosion near the channel axis, and thus form the symmetrical channel section, we introduce a small slope in the bottom profile (with an elevation difference of just 5 cm over L = 90 m). Because positions near the channel axis are slightly deeper, the flow starts to erode these positions first.

To resolve at each instant the equations presented above and find the bottom stresses, the simulation proceeds in the following way. Independent variables are discharge, water surface elevation, and bed geometry. We start with an initial energy slope S, then calculate using (9) the bottom stresses consistent with this energy slope and the known water depths. Using (6), we find the velocity distribution and, ultimately, the discharge. We then compare this discharge with the one assigned (spring discharge); if they do not coincide the energy slope S is corrected iteratively.

The simulation can be conduced with different discharges and different deposition and erosion periods. Here we illustrate three simulations. The first involves a constant discharge and homogeneous sediments, the second and the third involve an intermittent discharge with, respectively, homogeneous and stratified sediments.

3.1. Study Area

To simulate a realistic situation, we utilize data from Venice Lagoon. A detailed description of this environment is reported by *Fagherazzi et al.* [1999]. To specify the length L, we choose two adjacent salt marsh channels and take L as being equal to the distance between them (Figure 1). Upon specifying the watershed area A using the method described by *Rinaldo et al.* [1999a], together with the tidal amplitude [*Comune di Venezia,* 1999], we estimate with the continuity model an approximate spring tide discharge. The spring discharge is Q = 15 m^3 s^{-1}, the width of the channel is approximately w = 20 m, the depth d = 1.5 m, and the reference length L = 200 m. These values lead to a spring velocity peak of about v = 0.5 m s^{-1}, a value that is typical of salt marsh creeks [*Bayliss-Smith et al.*, 1979; *Healey et al.*, 1981; *French and Stoddart,* 1992].

For illustration we utilize (13) with a constant M = 1.4x10^{-3} kg m^{-2} s^{-1} [*Sanford and Halka,* 1993], consistent with experimental data [*Parchure and Mehta*, 1985; *Kuijper et al.*, 1989]. The dry density of the sediments is assumed to equal 400 kg m^{-3}, as reported for salt marshes in the Venice Lagoon by *Day et al.* [1998]. Here we assume a critical shear stress equal to τ_c = 0.4 N m^{-2}. This value is in agreement with flume data collected by *Parchure and Mehta* [1985] and *Kuijper et al.* [1989] for soft clay with the same dry density (400 kg m^{-3}) of the cohesive material collected in Venice Lagoon. The value assumed here is thus appropriate for soft cohesive sediments, although it may fail to characterize the behavior of well-consolidated cohesive sediments. We further suppose a constant deposition rate of 2 cm yr^{-1}, in agreement with field measurements in the Venice Lagoon [*Day et al.*, 1998]. We

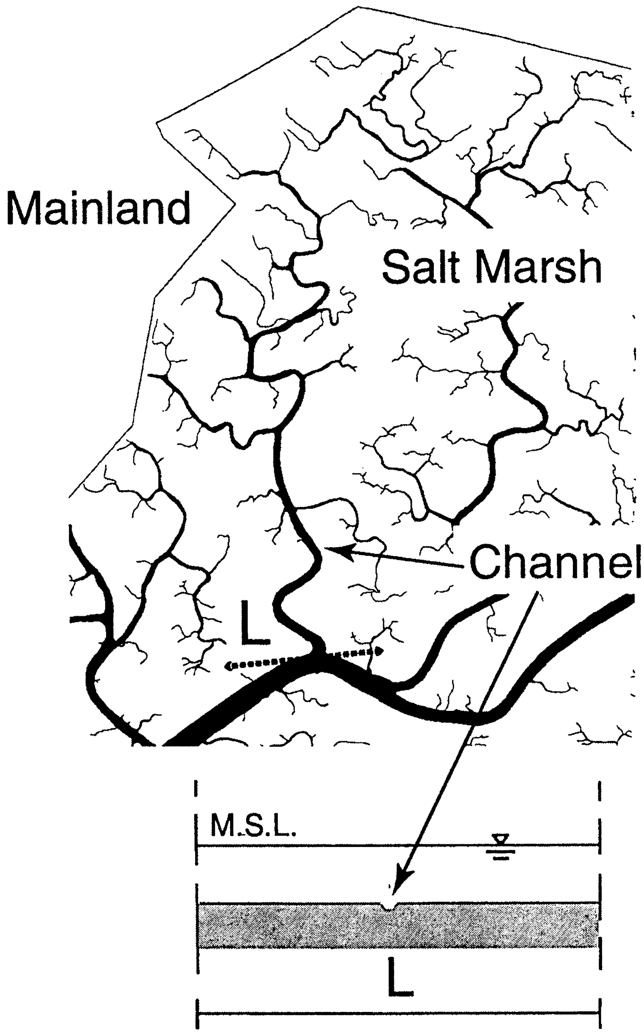

Figure 1. Sketch illustrating the geometry of the conceptual model for channel shape evolution. The channel chosen for the numerical example has been identified from aerial photographs of the northern part of the Venice Lagoon, 45° 30' Lat, 12° 24' Lon.

also suppose that, for a semidiurnal tide, the significant tidal discharge is a spring one, happening once each lunar month.

3.2. Constant Discharge

As previously described, an intermittent discharge with constant magnitude is consistent with the weak correlation between the exchange of water volume and bottom topography, an assumption that is valid for small, deep basins at early stages of salt marsh evolution, when the salt marsh surface is below mean sea level. The first simulation assumes steady constant discharge flowing in the reference cross section, fixed water surface level, and increasing bottom elevation.

This simulation will get insight into the channel formation, and it will be useful to explain the evolution considering an intermittent discharge. The fixed water surface level is imposed on the boundary by the ocean level. Furthermore, we initially consider homogeneous sediment material with constant erodibility.

Because an increase in bottom elevation due to sedimentation influences velocities and bottom shear stresses, the energy slope also increases to maintain the same specified discharge. When the critical stress is reached (starting near the channel axis) sedimentation is "stopped", and we allow erosion to occur until the bottom reaches an equilibrium configuration with shear stresses everywhere less than the critical stress (Figure 2). In this manner, depths, velocities, bottom stresses, and energy slope are allowed to differentially adjust over section L (Figure 3).

These simulations lead to the following behavior.

1. Following our conceptual model, a small increase in bottom elevation leads at some instant to a shear stress greater than the critical one over a part of L (see Figure 3b, $t = 0$ h).

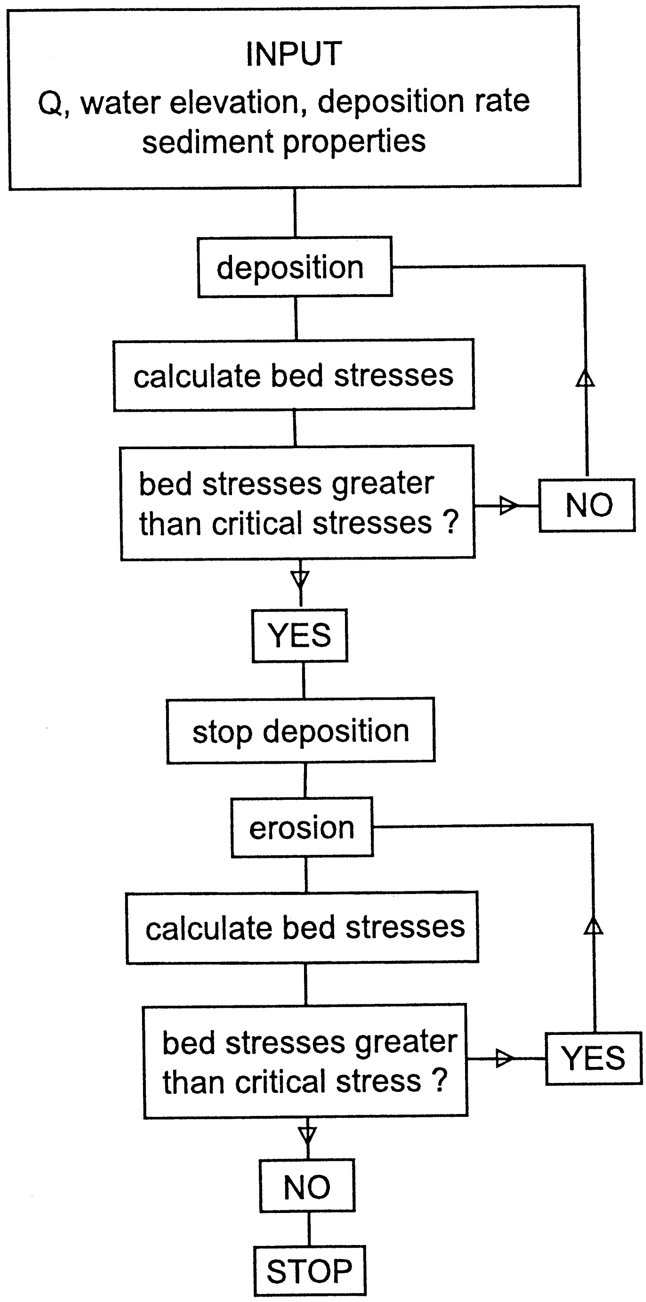

Figure 2. Flowchart for simulating channel incision with fixed constant water surface level and constant discharge.

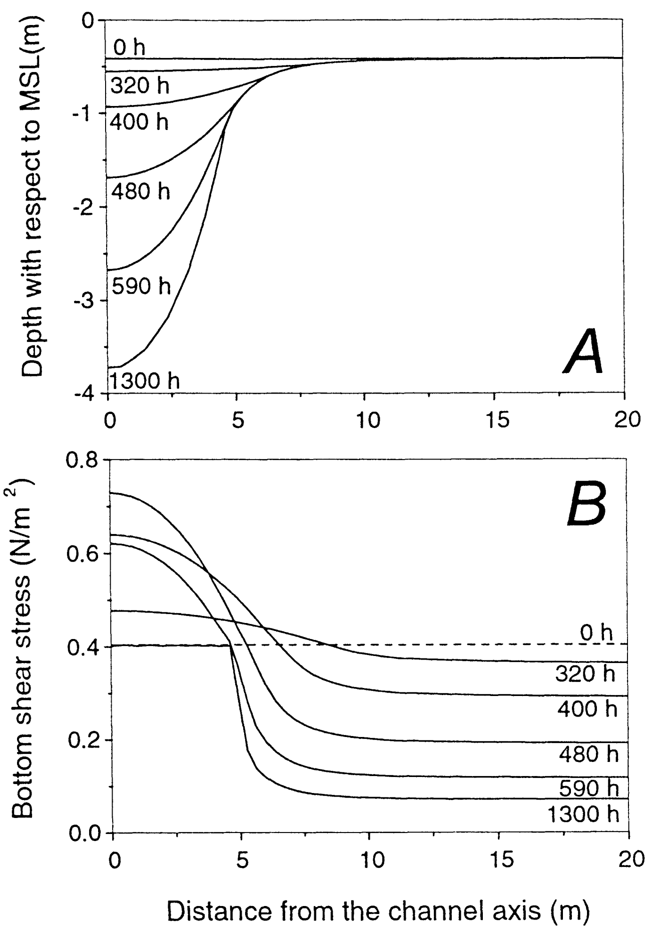

Figure 3. (a) Incision of the salt marsh channel caused by the redistribution of momentum from the salt marsh surface to the channel. The water surface level and the discharge are considered constant. The figure shows the channel geometry at different times. (b) Relative distribution of bottom shear stresses.

2. Here scour occurs near the symmetry axis. The shear stress is related through (4) to the ratio between the area dA and the wet perimeter dP, which in turn depends on the water depth y. Thus erosion is more pronounced near the symmetry axis, where the water depth is initially larger.
3. Two opposing mechanisms control the shear stress on that part of the bed that is subject to erosion. First, the increase in flow area leads to a decrease in energy slope, velocity, and bottom shear stress to maintain the same discharge. The second mechanism involves redistribution of momentum from the salt marsh surface to the part where the channel section is evolving. The concentration of flow in the channel part increases velocities and bottom shear stresses.
4. At early times of channel formation the second mechanism is stronger than the first one. For this reason the shear stress in the zone where erosion is localized increases until reaching a maximum (Figure 4a), and then it decreases toward the critical value associated with an equilibrium configuration. On the salt marsh surface adjacent to the channel, the shear stress is everywhere decreasing to maintain the constant discharge. Finally, the energy slope diminishes to allow a constant discharge in the section (Figure 4b).

These simulations suggest that the tidal channel forms due to the redistribution of momentum inside the section L associated with variations in the bottom topography, such that increasing differences in bottom topography provide a feedback mechanism that increases velocities and shear stresses in the deeper part.

In absence of a consideration of effects of bank stability on channel form, it is interesting to note that channel formation is mainly "vertical." That is, once the positions of "first scour" are determined, no new parts of the bottom are involved in scouring (Figure 3a). Initial differences in bottom elevation are accentuated during evolution, and the part of L subject to erosion becomes narrower with increasing (mean) depth. This means that a "front" of erosion migrates toward the channel axis, ceasing to exist when an equilibrium condition is achieved. At equilibrium the deeper part of the channel is at the critical shear stress (Figure 3b) such that the final state (Figure 3a) is a very deep creek. Thus a small initial variation in bottom elevation is sufficient to form a narrow, deep channel. If we allow the simulation to proceed unchecked, depositing further sediments, the depth of the channel increases to a point where normals to the bottom intersect so that the shear stress model becomes ineffective.

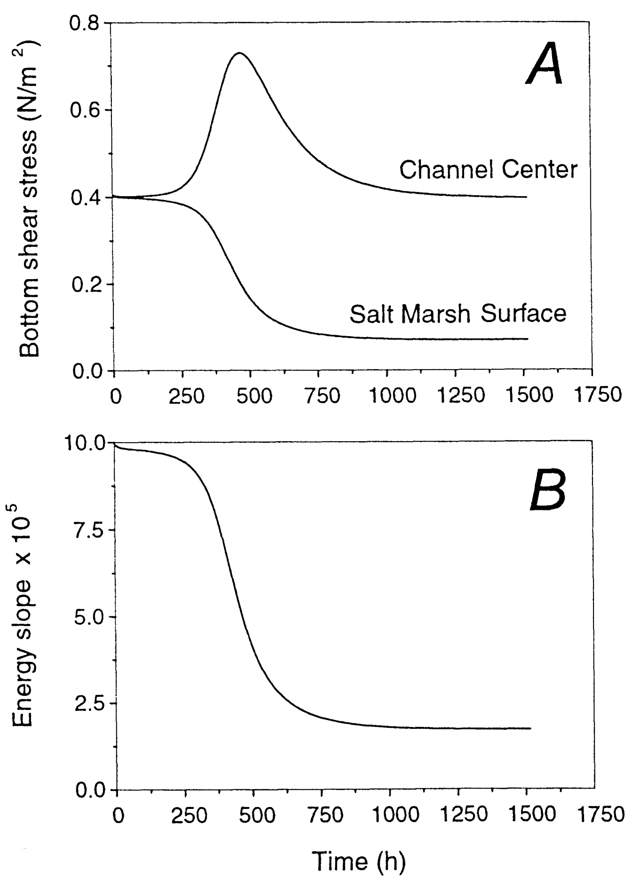

Figure 4. (a) Evolution of the bottom shear stress at the channel center and at the saltmarsh surface in function of time. The simulation refers to the situation described in Figure 3. (b) Energy slope evolution for the same simulation.

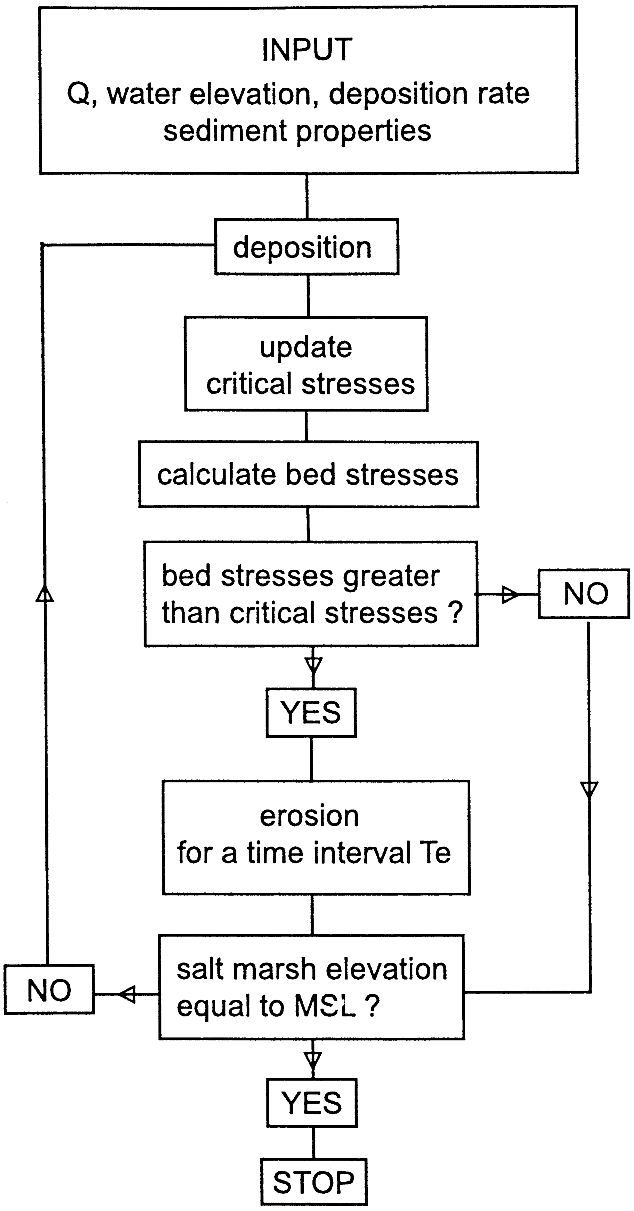

Figure 5. Flowchart for simulating channel incision with fixed constant water surface level, intermittent discharge, and increasing bottom elevation.

For this reason we stop our simulations after the first deposition that produces shear stresses higher than the critical one (Figure 3).

We note, however, certain deficiencies of this approach. First, the model of *Pizzuto* [1990] is valid for small curvature variations; when the channel becomes very deep the assumption of a logarithmic velocity profile along normals is not likely valid. Moreover, the section becomes compound, with well-developed channel and banks, where flow may become complex [*Shiono and Knight*, 1991]. For these reasons the results of the simulation should be viewed as providing a qualitative description of overall channel evolution.

3.3. Intermittent Discharge

In the previous section we noted that model simulations with steady constant discharge lead to narrow, deep channels that do not necessarily accord with observed width-depth ratios. Here we focus on a process that may play a major role in controlling channel cross-sectional shape in tidal environments: the fact that the geomorphically important discharge acts for a limited time. Based on typical erosion rates for cohesive sediments [*Sanford and Halka*, 1993; *Kuijper et al.*, 1989; *Parchure and Mehta*, 1985], we note that it would take aproximately 1300 hours of constant discharge to scour an equilibrium cross section, and approximately 500 hours to reach maximum values of shear stress, using the constant discharge model described previously (Figures 3 and 4). These timescales are unrealistic for salt marshes. If we assume, for example, that the spring tide provides the geomorphically important control on channel-network formation, the discharge caused by this tide flows in the channel just a few times every month and, for each time, it lasts a fraction of an hour [*Pestrong*, 1965; *Myrick and Leopold*, 1963; *Leopold et al.*, 1993]. However, the idea of a "geomorphic discharge" remains ambiguous. A tidal channel experiences continuously varying discharges, and it is debatable whether a single discharge level, or discharge interval, is dominantly responsible for channel shape.

Furthermore, cohesive sediments are subject to autoconsolidation, which leads to vertical variations in sediment density and erosion characteristics [*Cahoon and Reed*, 1995]. Variations in vertical density and erosion-threshold shear stress have been well studied in thin layers of deposited sediments. Within a few centimeters the sediment density can double and the threshold shear stress can triple [*Parchure and Mehta*, 1985; *Kuijper et al.*, 1989]. This behavior has a fundamental influence on the geomorphic shape of salt marsh creeks. In effect, as we illustrate below, erosion occurs only over the upper few centimeters of the sediments.

In this section we describe two sets of simulations. Both utilize an intermittent discharge that occurs for a specified duration T_e every month. In the first simulation the sediment is considered to be homogeneous with constant density and critical shear stress. In the second simulation a vertical change in density and critical stress is introduced to mimic effects of auto-consolidation.

The conceptual model for intermittent discharge is straighforward (Figure 5). At each time step corresponding to a lunar month a constant amount of material is deposited (1.7 mm in this example). The water surface elevation is maintained constant, and a reduction of liquid area due to deposition leads to an increase in bottom stresses. Bottom stresses are then updated. (As well, critical stresses in the simulation involving stratified sediments are updated.) If bottom stresses are greater than critical stresses, erosion occurs for a time interval equal to the duration of the geomorphic discharge (a few hours for a spring tide). The simulation is stopped when the elevation of that part of the salt marsh surface where erosion is not occurring reaches mean sea level. (This corresponds to about 25 years with an initial bottom elevation of 40 cm below MSL and a deposition rate of 2 cm yr^{-1}.)

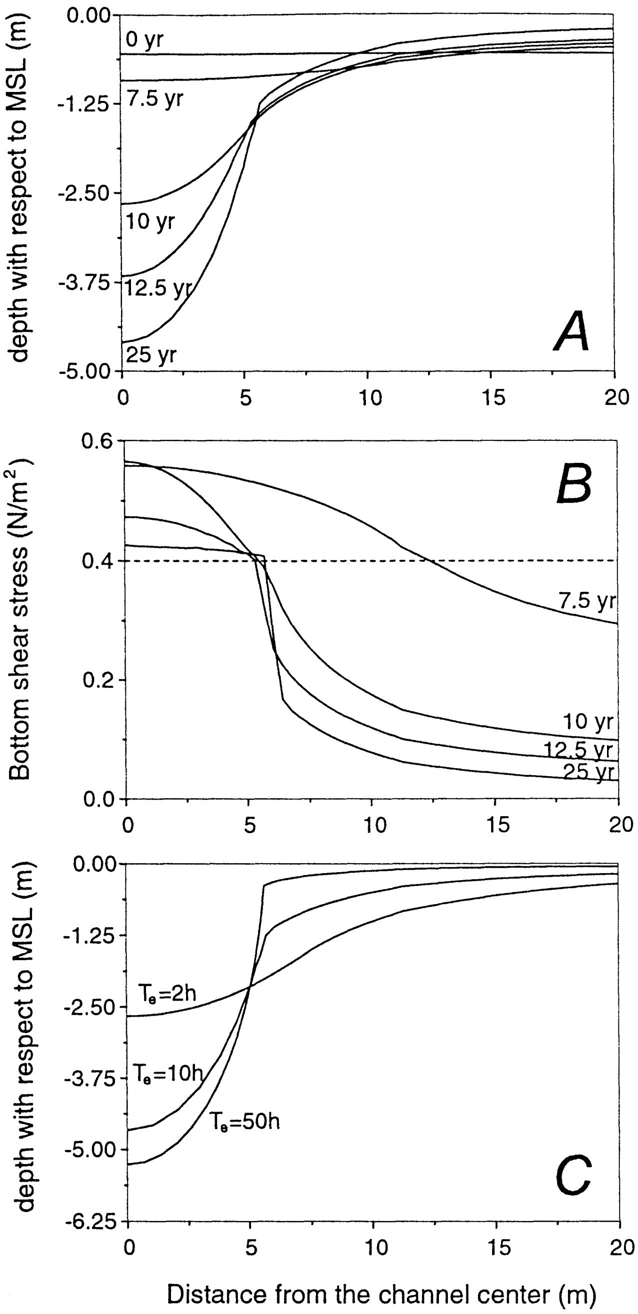

Figure 6. (a) Evolution of the channel geometry during the simulation with fixed constant water surface level, intermittent discharge, and increasing bottom elevation. (b) Relating shear stress distribution at the bottom. (c) Final channel configuration for different monthly duration T_e of the intermittent discharge.

3.3.1. Homogeneous Sediments. For the case of homogeneous sediments and a monthly flow duration of $T_e \cong$ 10 hours, no more than a few centimeters of scour occurs with a few millimeters of deposition each month. This intermittent discharge thus does not persist long enough for the channel cross section to reach a deep, narrow equilibrium configuration (Figure 6). As a consequence, the next (intermittent) discharge produces higher bed stresses over a larger portion of the section (Figure 6b after 7.5 years), and the channel becomes wider and shallower (Figure 6a). The adjustment toward an equilibrium configuration involves a larger part of the bottom, and the erosion front migrates slowly toward the channel axis.

At the end of the simulation the channel is wider and shallower than in the constant discharge simulation, with shear stresses at the bottom are slightly higher than the critical one (Figure 6b). By varying the flow duration T_e, the final bottom configuration also varies (Figure 6c). In particular, when the amount of material eroded each month is of the same magnitude or less than that deposited, the bottom shape becomes flat and gently sloped, because the flow does not have sufficient time to scour a deep channel. This situation exists in many wetland environments, where the salt marsh channels are weakly developed and slightly lower than the salt marsh surface. However, these channels extend into salt marshes with elevation above MSL, such that the reduction of the tidal prism and discharge has to be taken into account.

Another important item pertains to the asymptotic behavior of the salt marsh elevation [*Pethick*, 1981]. When the salt marsh elevation is close to or higher than MSL, the reduction in tidal prism and in the period of submergence slows deposition over the salt marsh. The creeks forming at this time then have more time to adjust toward the narrow, deep equilibrium configuration described in the previous section (Figure 3). Moreover, the larger channels in a network develop at the beginning of the salt marsh life, when sediment deposition is large and periods of scour are insufficient to produce deep channels, and so these larger channels are relatively wide. The flow instead needs shallow depths (correlated to high shear stresses) to form the smaller creeks. Thus they form in the mature period of the salt marsh in association with lower sedimentation rates, and they have a longer period to become deep. This may contribute to the disproportionate seaward widening of channels, relative to rivers, as reflected by the differences in their hydraulic geometries.

3.3.2 Sediment Stratification. Vertical changes in sediment characteristics may significantly influence channel cross-sectional shape. To illustrate this point, in view of the complexity of the deposition, consolidation process and the sparseness of field data necessary to fully characterize this process, we assume for simplicity that consolidation leads to a constant vertical gradient in sediment density and critical shear stress (even if vertical changes may be influenced by many factors [*Hayter*, 1986]). Although consolidation may take a nonnegligible time to develop, we further suppose that cohesive sediments adjust instantaneously to their density and critical shear stress as a function of the thickness of sediments above them. This hypothesis is supported by the fact that the estimated time for consolidation of cohesive sediments in salt marshes is of the same order (a few weeks) as the recurrence time of significant flows (spring tide) [*Hayter*, 1986; *Parchure and Mehta*, 1985; *Kuijper et al.*, 1989].

In the simulations, if the sediment has reached a specific density, this density is maintained (in absence of subsequent deposition or in presence of scour) or increased (with further deposition) but not decreased. The simulation thus checks at each point of the bed and for each time step the distance from the bed surface, then calculates the corresponding density and critical shear stress assuming a given vertical gradient in critical stress. Finally, it updates the bed characteristics,

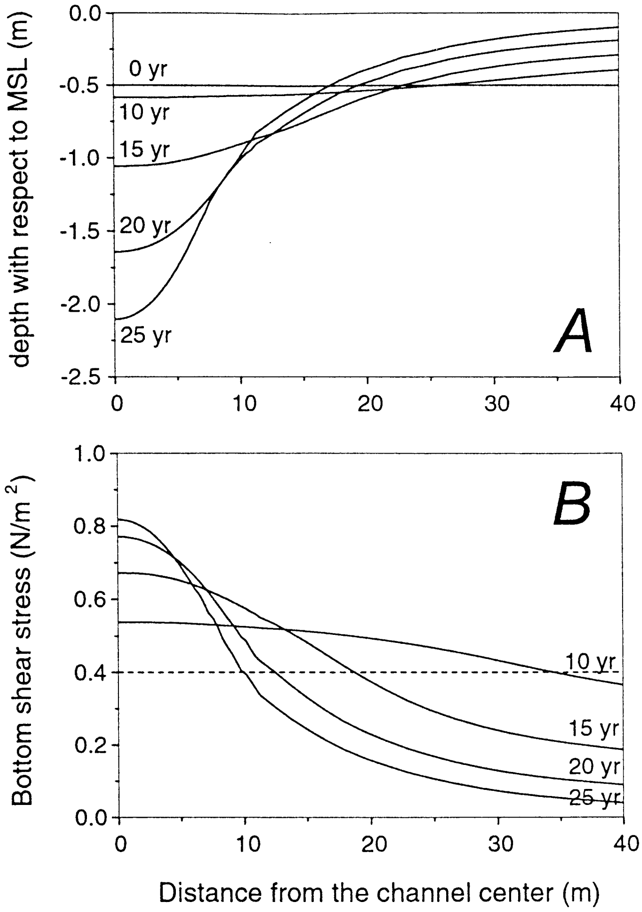

Figure 7. (a) Evolution of the channel geometry during the simulation with intermittent discharge and vertical increase in critical shear stress of the cohesive sediments deposited due to autoconsolidation. The vertical increase in critical shear stress is supposed to be equal to 0.133 N m^{-2} per m. (b) Relating shear stress distribution at the bottom.

checking that the critical shear stress and the density are not less than the actual one. Here we assume a vertical gradient in critical shear stress equal to 0.133 N m^{-2} m^{-1} and a density gradient equal to 200 kg m^{-3} m^{-1}. However, because we lack field data regarding vertical changes in sediment properties, a linear gradient is the simplest hypothesis, and the final configuration does not differ consistently from more complicated vertical distributions [e.g., *Hayter*, 1986].

The effects of vertical consolidation on channel shape are similar to those of intermittent discharges (Figure 7a). Namely, the flow encounters more resistant sediment layers over the entire section, and higher bottom shear stresses occur in the lateral zones where soft sediments can be easily removed. That is, a shear stress exceeding the critical one persists over a larger portion of the bottom (Figure 7b after 10 years), eroding a wider channel section. The shear stress at the center of the channel continues to grow with time, because the flow erodes to more resistant layers which allow higher values of stress. At the end of the simulation the channel shape (Figure 8a) is realistic, with a depth of 2 m and a width of 20 m. Dotted lines in Figure 8a represent surfaces having constant sediment density and constant critical shear stress. It is evident from these that, during its development, the channel cuts layers with different mechanical properties. The higher position of isolines of critical stress beneath the salt marsh surface, relative to the position beneath the channel, is due to the lack of erosion in this zone, and the consequent greater thickness of the sediment. A sensitivity analysis involving different vertical gradients in critical stress further suggests a strong influence of vertical changes in sediment characteristics (Figure 8b). Small differences in vertical properties change the erosion sedimentation mechanism and the linked channel cross section. For high shear stress gradients the channels are wide and shallow with gentle slope; for low gradients the channels are narrow and deep.

Stephens et al. [1992] collected measurements of bulk sediment properties in a muddy macrotidal estuary. The bottom bulk density and the critical erosive shear stress of the upper layer of the sediments show a linear decay upstream from the estuary mouth. A similar trend should be expected in salt marsh environments. In the upper reaches of a salt marsh network, where discharges are relatively small, flows are likely to erode only the surficial bed layers. Near the mouth, relatively larger discharges conveyed by the network are able to remove more material at the bottom, reaching

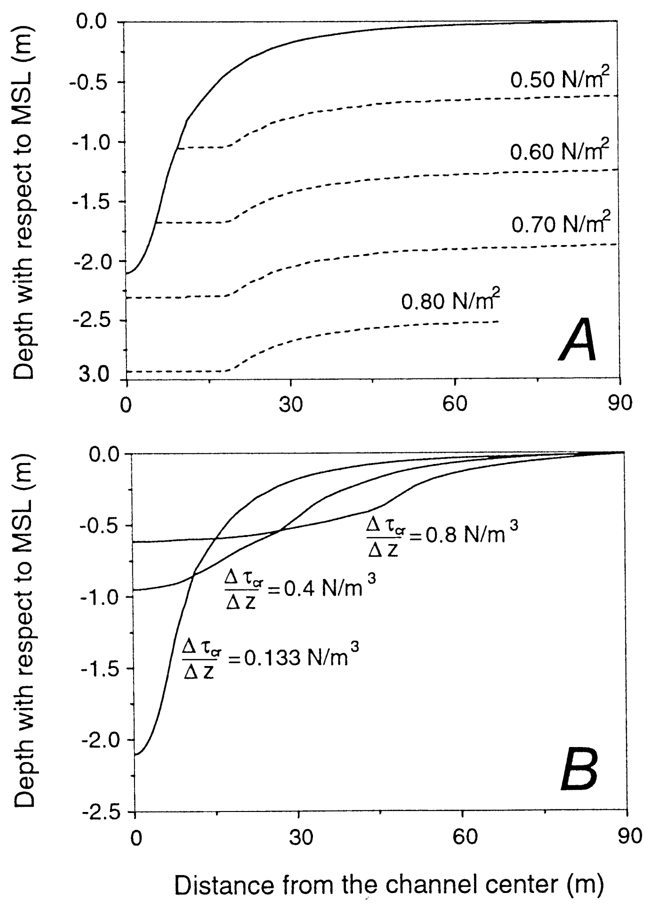

Figure 8. a) Final configuration of the channel bottom for the simulation described in Figure 7. The dotted lines show the points in deposited sediments having the same critical shear stress. b) Final bottom configuration with different vertical gradients of critical shear stress due to autoconsolidation of the cohesive sediments.

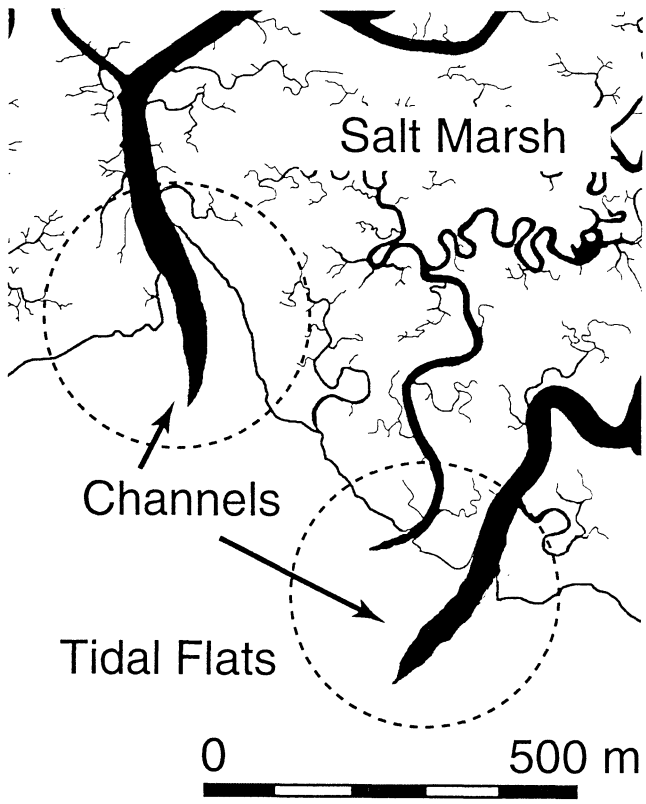

Figure 9. Salt marsh channels cutting the adjacent tidal flat. The cutting phenomenon is due to incision of preexisting sediment layers and is predicted by the model delineated in the text. The salt marsh is in the northern part of the Venice Lagoon (45° 30' Lat, 12° 24' Lon), and the channels are identified from aerial photographs.

deeper, more resistant layers. Note, however, that the data collected by *Stephens et al.* [1992] refer to an estuary, where the length scale is much longer than the typical length scale of salt marshes and the geomorphological evolution can be different, and not linked to the deposition mechanism described here. Nevertheless, we suspect that empirical evidence in salt marshes should show the same behavior. For similar reasons, a lateral variation (between the channel bottom and the salt marsh surface) in sediment properties should occur (Figure 8a). Namely, sediment should be softer on the salt marsh surface where erosion does not occur and deeper, stronger sediments are not exhumed.

Creek formation via downward erosion into older sediment layers is well illustrated in the salt marshes of Venice Lagoon. For example, surveys of salt marsh creek networks in the northern part of the Venice Lagoon (Regione Veneto) clearly show that, at the border between salt marsh and tidal flats, creeks are deeper than the bottom elevation of the tidal flat, having cut into the tidal flat bottom for several decimeters (Figure 9, circled area).

Abrupt changes in sediment composition can also influence channel shape. *Rinaldo et al.* [1999a] showed the presence of breaks in a log-log diagram linking channel width with peak discharge. The model herein can conceptually explain these breaks as being the result of channel formation involving cutting through different sediment layers with distinct erodibilities. Changes in sediment composition are moreover well documented in the Venice Lagoon salt marshes [*Colombo and Matteotti*, 1963; *McClennen et al.*, 1997], where silty clay grades to silty sand in the deeper layers.

4. Conclusions

In this contribution a new morphological model able to study cross-sectional evolution of salt marsh channels is presented. The high complexity involved in the salt marsh morphodynamics, complexity due to the difficulty in characterizing tidal flow in this environment combined with the lack of knowledge about the sediment transport behavior, suggests to simplify the problem in order to underline the processes chiefly responsible of the creeks shape and development. Here simplified hydrodynamic assumptions lead to a flexible cross-sectional model able to study the influences of different geological processes on channel shape. A key assumption regards the deposition process, considered to be uniform spatially. This assumption limits the applicability of the model to salt marsh formation. The flow is treated as a sequence of determined discharges flowing in a reference cross section with bottom topography dictated by the erosion deposition process. The model is straightforward in following creek evolution in the first stages of the salt marsh, where modifications in tidal prism are negligible.

In particular, two major causes of creek widening in salt marshes are presented. In contrast with terrestrial rivers, salt marsh creeks experience a strong increase of width-depth ratio in the seaward direction. The short duration time of the peak discharge (and the consequent erosion scale comparable with the deposition scale) is responsible of this widening. The creek cross section has not time to adjust itself, through the erosion process, toward a narrow and deep equilibrium configuration. Moreover, the autoconsolidation of the bottom cohesive sediments and the consequent vertical gradients in resistance properties obstructs the formation of deep creeks, yielding the formation of shallow wide channels.

The hypotheses adopted in this paper confine its application to youthful salt marsh development. The following step toward the construction of a three-dimensional salt marsh evolution model will be the extension of this model to mature salt marshes, were salt marsh accretion causes a decrease in tidal prism which influences directly sediment supply and discharges flowing in the creek network. Furthermore, in mature salt marshes, vegetation plays a fundamental role in salt marsh surface stabilization.

Acknowledgments. This paper benefited from suggestions of William E. Dietrich and Stuart Siegel (University of California at Berkeley). We also thank Andrea Rinaldo, Marco Marani and Stefano Lanzoni (Universita' di Padova) for enlightening discussions. The first author gratefully acknowledges support provided by Fondazione Aldo Gini, Padova, Italy, the University of Padova through the scholarship Borse di studio per la frequenza di attivita' di perfezionamento all'estero, and by the School of Computational Science and Information Technology, Florida State University.

References

Allen, J.R.L., Salt marsh growth and stratification: A numerical model with special reference to the Severn Estuary, southwest Britain, *Mar. Geol.*, *95*, 77-96, 1991.
Allen, J.R.L., Salt marsh growth and fluctuating sea level:

Implications of a simulation model for Flandrian coastal stratigraphy and peat-based sea-level curves, *Sediment. Geol., 100*, 21-45, 1995.

Allen, J.R.L., Simulation models of salt marsh morphodynamics: Some implications for high-intertidal sediment couplets related to sea-level change, *Sediment. Geol., 113*, 211-223, 1997.

Ariathurai, C.R., and R.B. Krone, Finite element model for cohesive sediment transport, *J. Hydraul. Div. Am. Soc. Civ. Eng., 103*(3), 323-338, 1976.

ASCE Task Committee on Erosion of Cohesive Materials Committee on Sedimentation, Erosion of cohesive sediments *J. Hydraul. Div. Am. Soc. Civ. Eng., 94*(HY4), 1017-1049, 1968.

ASCE Task Committee on Hydraulics, Bank Mechanics, and Modelling of River Width Adjustment, River width adjustment, I, Processes and mechanisms, *J. Hydraul. Div. Am. Soc. Civ. Eng., 124*(9), 881-992, 1998a.

ASCE Task Committee on Hydraulics, Bank Mechanics, and Modelling of River Width Adjustment, River width adjustment, II, Modeling, *J. Hydraul. Div. Am. Soc. Civ. Eng., 124*(9), 903-917, 1998b.

Bayliss-Smith, T.P., R. Healey, R. Lailey, T. Spencer, and D.R. Stoddart, Tidal flows in salt marsh creeks, *Estuarine Coastal Mar. Sci., 9*, 235-255, 1979.

Blondeaux, P., and G. Seminara, A unified bar-bend theory of river meanders, *J. Fluid Mech., 157*, 449-470, 1985.

Boon, J.D., III, Tidal discharge asymmetry in a salt marsh drainage system, *Limnol. Oceanogr., 20*, 71-80, 1975.

Bruun, P., *Stability of Tidal Inlets*, Elsevier Sci., New York, 1978.

Cahoon, D.R., and D.J. Reed, Relationships among marsh surface topography, hydroperiod, and soil accrection in a deteriorating Louisiana salt marsh, *J. Coastal Res., 11*(2), 357-369, 1995.

Collins, M.B., X. Xe, and S. Gao, Tidally-induced flow structure over intertidal flats, *Estuarine Coastal Shelf Sci., 46*, 233-250, 1998.

Colombo, P.,and G. Matteotti, Contributo allo studio delle caratteristiche geotecniche dei terreni della Laguna di Venezia e zone limitrofe, Atti dell' Istituto Veneto Sci., lett., Arti, Tomo CXXI, Venice, 1963.

Comune di Venezia, Previsioni delle altezze di marea per il bacino di San Marco e delle velocita' di corrente per il Canal Porto di Lido - Laguna di Venezia, in Valori astonomici, 181 pp., Poligrafico dello Stato, Rome, 1999.

Day, J.W., Jr., A. Rismondo, F. Scarton, D. Are, and G. Cecconi, Relative sea level rise and Venice lagoon wetlands, *J. Coastal Conserv., 4*, 27-34, 1998.

Delo, E.A., Estuarine mud manual, *Rep. SR164*, 31 pp., Hydraul. Res., Wallinford, England, 1988.

Diplas, P., and G., Vigilar, Hydraulic geometry of threshold channels, *J. Hydraul. Div. Am. Soc. Civ. Eng.*, 118(4), 597-614, 1992.

Dronkers, J.J., *Tidal Computations*, 518 pp., North-Holland, New York, 1964.

Dyer, K.R., Current velocity profiles in a tidal channel, *Geophys. J. R. Astron. Soc., 22*, 153-161, 1970.

Dyer, K.R., Sediment transport processes in estuaries *Geomorphology and Sedimentology of Estuaries, Developments in Sedimentology*, edited by G.M.E. Perillo, Elsevier Sci., New York, 1995.

Einstein, H.A., The bed-load function for sediment transportation in open channel flows, *Tech. Bull.*, 71 pp., U.S. Dep. of Agric., Washington, D.C., 1950.

Fagherazzi S., A. Bortoluzzi, W.E. Dietrich, A. Adami, S. Lanzoni, M. Marani, and A. Rinaldo, Tidal networks, 1, Automatic network extraction and preliminary scaling features from DTMs, *Water Resour. Res., 35*(12), 3891-3904, 1999.

French, J.R., Numerical simulation of vertical marsh growth and adjustment to accelerated sea-level rise, North Norfolk, U.K., *Earth Surf. Processes Landforms, 18*, 63-81, 1993.

French, J.R. and D.R. Stoddart, Hydrodynamics of saltmarsh creek systems: implications for marsh morphological development and material exchange, *Earth Surf. Processes Landforms, 17*, 235-252, 1992.

Friedrichs, C.T., Stability shear stress and equilibrium cross-sectional geometry of sheltered tidal channels, *J. Coastal Res., 11*(4), 1062-1074, 1995

Friedrichs, C.T. and D.G. Aubrey, Tidal propagation in strongly convergent channels, *J. Geophys. Res., 99*(C2) 3321-3336, 1994

Gabet, E.J., Lateral migration and bank erosion in a saltmarsh tidal channel in San Francisco Bay, California, *Estuaries, 4B*, 745-753, 1998.

Gardner, L.R. and M. Bohn, Geomorphic and hydraulic evolution of tidal creeks on a subsiding beach ridge plain, North Inlet, S.C., *Mar. Geol., 34*, M91-M97, 1980.

Garofalo, D., The influence of wetland vegetation on tidal stream channel migration and morphology, *Estuaries, 3*(4), 258-270, 1980.

Hayter, E.J., Estuarial sediment bed model, *in Lecture Notes on Coastal and Estuarine Studies*, edited by A.J. Mehta, Springer-Verlag, New York, 1986

Healey, R.G., K. Pye, D.R. Stoddart, and T.P. Bayliss-Smith, Velocity variation in salt marsh creeks, Norfolk, England, *Estuarine Coastal Shelf Sci., 13*, 535-545, 1981.

Henderson, F.M., *Open Channel Flow*, 522 pp., Macmillan, Indianapolis, Ind., 1966.

Kovacs, A., and G. Parker, A new vectorial bedload formulation and its application to the time evolution of straight river channels, *J. Fluid Mech., 267*, 153-183, 1994.

Krone, R.B., A method for simulating historic marsh elevations, in *Coastal Sediments '87*, edited by N.C. Kraus, pp. 316-323, Am. Soc. of Civ. Eng., Reston, Va., 1987.

Krone, R.B., Sedimentation revisited, in *Nearshore and Estuarine Cohesive Sediment Transport*, Coastal Estuarine Stud. Ser., vol. 42, edited by A.J. Mehta, pp. 108-125, AGU, Washington, D.C., 1993.

Kuijper, C., J.M. Cornelisse, and J.C. Winterwerp, Research on erosive properties of cohesive sediments, *J. Geophys. Res., 94*, 14,341-14,350, 1989.

Lanzoni, S., and G. Seminara, On tide propagation in convergent estuaries, *J. Geophys. Res.*, 103, 30,793-30,812, 1998a.

Lanzoni, S., and G. Seminara, Sull'equilibrio morfodinamico degli estuari, in *XXVI Convegno di Idraulica e costruzioni Idrauliche, Vol. I*, pp. 333-344, Catania 1998b.

Leopold, L.B., and T. Maddock Jr., The hydraulic geometry of stream channels and some physiographic implications, *U.S. Geol. Surv. Prof. Pap. 252*, 1953.

Leopold, L.B., J.N. Collins, and L.M. Collins, Hydrology of some tidal channels in estuarine marshlands near San Francisco, *Catena, 20*, 469-493, 1993.

Lundgren, H. and Jonsson, I.G., shear velocity distribution in shallow channels, *J. Hydraul. Div. Am. Soc. Civ. Eng., 90*(HY1), 1-21, 1964.

Lynn, A.L., A.C. Hine, and M.E. Luther, Surficial sediment transport and deposition processes in a Juncus roemerianus marsh, West-Central Florida, *J. Coastal Res., 11*(2), 322-336, 1995.

Maas, L.R.M., On the nonlinear Helmholtz response of almost-enclosed tidal basins with sloping bottoms, *J. Fluid Mech., 349*, 361-380, 1997.

McClennen, C.E., A.J. Ammerman, and S.G. Schock, Framework stratigraphy for the Lagoon of Venice, Italy: Revealed in new seismic-reflection profiles and cores, *J. Coastal Res., 13*(3), 745-759, 1997.

Mehta, A.J., E.J. Hayter, W.R. Parker, R.B. Krone, and A.M. Teeter, Cohesive sediment transport, I, Process description *J. Hydraul. Div. Am. Soc. Civ. Eng., 115*(8), 1076-1093, 1989.

Myrick, R.M. and L.B. Leopold, Hydraulic geometry of a small tidal estuary. *U.S. Geol. Surv. Prof. Pap. 422-B*, 18, 1963.

Parchure, T.M., and A.J. Mehta, Erosion of soft cohesive sediment deposits, description *J. Hydraul. Div. Am. Soc. Civ. Eng., 111*(10), 1308-1326, 1985.

Pestrong, R., The development of drainage patterns on tidal marshes, *Stanford Univ. Publ. Geol. Sci., Tech. Rep. 10*, 87, 1965.

Pethick, J.S., Velocity surges and asymmetry in tidal channels, *Estuarine Coastal Mar. Sci., 11*, 331-345, 1980.

Pethick, J.S., Long-term accretion rates on tidal salt marshes, *J. Sediment. Petrol., 51*(2), 571-577, 1981.

Pizzuto, J.E., Numerical simulation of gravel river widening, *Water Resour. Res., 26*(9), 1971-1980, 1990.

Redfield, A.C., Development of a New England salt marsh, *Ecol. Monogr., 24*(2), 201-237, 1972.

Rinaldo, A., S. Fagherazzi, S. Lanzoni, M. Marani, and W.E. Dietrich, Tidal networks, 2, Watershed delineation and comparative network morphology, *Water Resour. Res. 35*(12), 3905-3917, 1999a.

Rinaldo, A., S. Fagherazzi, S. Lanzoni, M. Marani, and W.E. Dietrich, Tidal networks, 3, Landscape-forming discharges and studies in empirical geomorphic relationships, *Water Resour. Res. 35*(12), 3919-3929, 1999b.

Sanford, L.P., and J.P. Halka, Assessing the paradigm of mutually exclusive erosion and deposition of mud, with examples from upper Chesapeake Bay, *Mar. Geol., 114*, 37-57, 1993.

Shiono, K., and D.W. Knight, Turbulent open-channel flows with variable depth across the channel, *J. Fluid Mech., 222*, 617-646, 1991.

Shuttelaars, H.M., and H.E. De Swart, An idealized long-term morphodynamic model of a tidal embayment, *Eur. J. Mech. B/Fluids, 15*(1), 55-80, 1996.

Stephens, J.A., R.J. Uncles, M.L. Barton, and F. Fitzpatrick, Bulk properties of intertidal sediments in a muddy, macrotidal estuary, *Mar. Geol., 103*, 445-460, 1992.

Van Eerdt, M.M., Salt marsh cliff stability in the Oosterschelde, *Earth Surf. Processes Landforms, 10*, 95-106, 1985.

Woolnough, S.J., J.R.L. Allen, and W.L. Wood, An exploratory numerical model of sediment deposition over tidal salt marshes, *Estuarine Coastal Shelf Sci., 41,* 515-543, 1995.

S. Fagherazzi, School of Computational Science and Information Technology, Florida state University, 150 Dirac Science Center Library, Tallahassee, FL 32306-4120. (sergio@csit.fsu.edu). D.J. Furbish, Department of Geological Sciences and Geophysical Fluid Dynamics Institute, Florida State University, Tallahassee, FL 32306-4100. (furbish@gly.fsu.edu).

(Received November 3, 1999; revised June 9, 2000;
accepted September 6, 2000.)